

# Replacing sulfonate by carboxylate: Application of pyridyliminocarboxylato copper(II) complexes in *rac*-lactide polymerization and Chan-Evans-Lam coupling.

*Valérie Hardouin Duparc, Clémentine Dimeck, Frank Schaper\**

Centre in Green Chemistry and Catalysis, Département de chimie, Université de Montréal, 2900  
Boul. E.-Montpetit, Montréal, QC, H3T 1J4, Canada

\* Frank.Schaper@umontreal.ca

## **Author email addresses :**

Valérie Hardouin Duparc : valerie.hardouin.duparc@gmail.com

Clémentine Dimeck : clementine.dim@outlook.fr

Frank Schaper : Frank.Schaper@umontreal.ca

## Abstract

Copper(II) complexes carrying pyridylmethyleaminobenzoate or -propanoate ligands, LCuX, were prepared in one-pot reactions from pyridinecarboxaldehyde, aminobenzoic acid or  $\beta$ -alanine, and CuX<sub>2</sub> (X = Cl, NO<sub>3</sub>, OAc or OTf). All complexes were characterized by single-crystal X-ray diffraction studies and formed either dimers, tetramers or coordination polymers. Attempted preparation of the respective alkoxide complexes, LCu(OR), was unsuccessful, but use of LCuX/NaOMe mixtures in *rac*-lactide polymerization indicated under some conditions coordination-insertion polymerization via a copper alkoxide as the mechanism. The complexes performed poorly in *rac*-lactide polymerization, showing low activities (12 h to completion at 140 °C), low to moderate heterotacticity ( $P_r = 0.6-0.8$ ) and poor polymer molecular weight control (intramolecular transesterification). They were competent catalysts for Chan-Evans-Lam couplings with phenylboronic acid, without any indication of side reactions such as deboration or aryl homocoupling. The complexes were active in undried methanol, without addition of base, ligand or molecular sieves. Aniline, *n*-octylamine and cyclohexylamine were coupled quantitatively under identical reaction conditions. There is only little influence of the anion on activities (less than a factor of 2), but a strong influence on induction periods. The complexes were not active in CEL coupling with alcohols, phenols, or alkylboronic acids.

*Copper complexes, homogenous catalysis, Chan-Evans-Lam coupling, lactide polymerization, mechanism*

## Introduction

Copper has found widespread use in catalytic transformations,<sup>1,2</sup> but its application in polymerization catalysis caused some controversy. It has been widely employed in radical polymerizations involving a Cu(I)/Cu(II) redox couple,<sup>3-4</sup> but much less in homogenous, 2-electron processes. Copper(II) diimine complexes have been reported to copolymerize ethylene and methacrylate by a coordination-insertion mechanism.<sup>5-7</sup> However, the very low activity of the system and the lack of a convincing mechanism make it doubtful that copper(II) does indeed polymerize ethylene. Radical mechanisms, involving copper(I) or ligand transfer to a catalytically active Al-species have been proposed as potential alternative reaction pathways.<sup>8-9</sup> Cu(II) complexes have also been claimed to polymerize acrylonitrile via a coordination-insertion mechanism,<sup>10</sup> but again this was doubted later and a different mechanism, not involving Cu(II), was proposed to be responsible for the observed results.<sup>11</sup> There is no doubt, however, that Cu(II) complexes are active in the ring-opening polymerization of lactide to polylactic acid (PLA).

There is currently significant interest in the controlled polymerization of lactide,<sup>12-31</sup> but efforts have been concentrated for the most part on catalysts based on groups 1-4 and 12-14. In the limited number of copper-catalyzed reactions, polymerizations proceeded either via Lewis-acid activation of the monomer,<sup>32-41</sup> or via insertion into a copper-alkoxide bond.<sup>42-53</sup> We have previously reported that diketiminate copper alkoxides provide highly active, but controlled polymerization catalysts.<sup>51-53</sup> They are, however, very sensitive to air and moisture, which severely limits their applicability. To provide copper(II) polymerization catalysts with a ligand framework less susceptible to oxidation and hydrolysis, we recently investigated copper complexes with sulfonate-based ligands (Scheme 1, **A - C**). The sulfonate complexes proved to be unsuitable for lactide polymerization: the respective alkoxide complexes could not be isolated or – based on polymerization results – not even be prepared in situ.<sup>54-55</sup> They proved to be, however, highly competent catalysts for Chan-Evans-Lam couplings of *N*-nucleophiles.<sup>54-57</sup> Chan-Evans-Lam couplings are oxidative, copper-catalyzed couplings between a boronic acid and a second nucleophile, with copper(II) acetate being the most widely employed catalyst.<sup>58-60</sup> Compared to the Ullmann-Goldberg reaction or Buchwald-Hartwig aminations catalyzed by palladium or copper, CEL couplings proceed under much milder conditions, often at room temperature, and are thus more attractive for complicated and sensitive substrates.<sup>61-72</sup> Complexes **A-C**, but in particular **B**, showed quantitative

conversion of amines, anilines and *N*-heterocycles using an identical reaction protocol and requiring a minimum of optimization of reaction conditions.<sup>54-57</sup>

Based on the assumption that one reason for the instability of  $(L_{\text{sulfonate}})Cu(OR)$  in lactide polymerization is related to desulfonation, we investigated analogs to **B** and **C**, replacing the sulfonate group with carboxylate (**D** and **E**, Scheme 1), as catalysts in lactide polymerization. In Chan-Evans-Lam (CEL) couplings, the sulfonate group of **A-C** was proposed to bridge to boron in an intermediate dinuclear complex prior to transmetallation. Complexes **D** and **E** were thus also investigated for CEL couplings to test whether the carboxylate group is capable of providing the same functionality. Complexes  $(L1)CuX$ , **D**, have been previously prepared by Mitra and coworkers with oxalate, nitrate/azide and fluoroacetate anions.<sup>73-75</sup>  $[(L2)Cu]X$ , **E**, has been reported with  $X = \text{oxalate, azide or nitrate}$ .<sup>76-79</sup> To allow comparisons with the respective sulfonate complexes, we targeted complexes with chloride, nitrate, acetate and triflate counteranions.

## Results and Discussion

**Ligand syntheses.** Our attempts to prepare **L1H** following literature protocols<sup>75</sup> did not afford a clean product.<sup>80</sup> Best results in optimizing ligand synthesis were obtained by using a Dean-Stark apparatus to eliminate water or microwave reactions in the presence of molecular sieves, both of which afforded 80% conversion. Despite numerous attempts, conversion could not improved any further. Attempts to purify the ligand were not successful and at best 95% purity according to NMR could be obtained. Preparation of  $\beta$ -alanine-based ligand **L2H** has not been reported and attempts similar to the synthesis of **L1H** failed. While we cannot exclude a simple experimental problem on our side, the analogous sulfonate-based ligands were reported to be highly sensitive to hydrolysis.<sup>79</sup> On the other hand, they assemble readily to the ligand in the presence of a metal center to provide the respective metal complex.<sup>81</sup> **L1H** (95% purity) was thus employed for the attempted preparation of alkoxide complexes, while copper complexes with **L1** or **L2** ligands and other anions were obtained by direct condensation of the ligand on the metal center (Scheme 2).

**Complex syntheses.** Reaction of anthranilic acid with pyridinecarbaldehyde and copper(II) chloride in methanol cleanly provided  $(L1)CuCl \cdot H_2O$ , **1**, which crystallized as the dinuclear chloride bridged complex (Scheme 3, Table 1, Fig. 1). The coordination geometry around

copper is square-pyramidal ( $\tau = 0.0$ ) with **L1** and chloride in the equatorial plane and the bridging chloride in the apical position with an elongated ( $\Delta d = 0.4 \text{ \AA}$ ) bond to copper. The structure of carboxylate complex **1** is very similar to the respective sulfonate complex **B** (Table 1). The only difference is the twisting of  $30^\circ$  between the aryl and the pyridyl rings in **B**, required by the tetrahedral geometry of the sulfonate group, (only  $5^\circ$  in **1**) and a very slightly shorter Cu-O distance ( $\Delta d = 0.06 \text{ \AA}$ ) for carboxylate vs. sulfonate coordination. Since the presence of co-crystallized water might prevent preparation of alkoxide complexes, **1** was recrystallized in dry methanol to provide  $(\mathbf{L1})\text{CuCl}\cdot\text{MeOH}$ , **2**, which is isostructural with water replaced by methanol (Scheme 3, Fig. 1, Table 1).

**Table 1.** Selected geometric data of X-ray structures of **1-5**

	<b>B</b> <sup>a</sup>	<b>1</b>	<b>2</b>	<b>3</b>	<b>4</b>	<b>5</b>
Cu-O <sub>2</sub> C	1.964(2)	1.891(1), 1.905(1)	1.892(6), 1.900(6)	1.942(4) – 1.954(4)	1.894(1)	1.926(3)
Cu-N(=C)	2.068(2)	2.020(2), 2.003(2)	2.020(7), 2.015(7)	1.968(5) – 1.980(5)	1.996(2)	1.998(3)
Cu-N <sub>pyridine</sub>	2.002(2)	2.002(2), 2.003(2)	2.020(7), 1.998(7)	2.008(5) – 2.025(5)	1.988(2)	1.983(4)
Cu-OH <sub>2</sub>				2.153(5) – 2.168(5)		2.200(4)
Cu-X <sup>b</sup>	2.276(1)	2.287(2), 2.305(2)	2.305(3), 2.306(2)		1.973(1)	
Cu-L <sup>b</sup>	2.679(1)	2.720(2), 2.660(2)	2.676(3), 2.656(2)	1.935(4) – 1.941(4)	2.295(2)	1.950(3)
$\tau$	0.0	0.1, 0.1	0.1, 0.1	0.5	0.1	0.0

<sup>a</sup> Data taken from ref. <sup>82</sup> <sup>b</sup> **B**, **1**, **2**: X= $\mu$ -Cl<sub>short</sub>, L= $\mu$ -Cl<sub>long</sub>. **3**: L= $\mu$ -CO<sub>2</sub>. **4**: X= $\mu$ -OAc<sub>short</sub>, L= $\mu$ -OAc<sub>long</sub>. **5**: L= $\mu$ -O<sub>2</sub>CR

Reactions in the presence of copper nitrate or copper acetate yielded the respective complexes  $[(\mathbf{L1})\text{Cu}(\text{OH}_2)][\text{NO}_3]\cdot\text{H}_2\text{O}$ , **3**,<sup>75</sup> and  $(\mathbf{L1})\text{Cu}(\text{OAc})\cdot 2\text{H}_2\text{O}$ , **4**, both with co-crystallized/coordinated water (Scheme 3, Table 1, Fig. 1). Recrystallization in dry methanol to remove water failed in these cases. Complex **3** crystallizes as a tetramer in the structure described previously.<sup>75, 83</sup> Acetate complex **4** crystallizes as a dimeric complex with bridging acetate ligands. Surprisingly, the acetate shows a monodentate coordination to the copper centres instead of the more common bidentate bridging mode and is structurally very similar to the chloride-bridged complex **1** or **2**. The triflate complex  $[(\mathbf{L1})\text{Cu}(\text{OH}_2)][\text{OTf}]$ , **5**, can be

obtained by either anion exchange from **1** with AgOTf or by direct reaction of copper(II) triflate with the ligand precursors (Scheme 3). In both cases, the complex crystallizes as a 1D coordination polymer (Fig. 1). A bridging carboxylate replaced the triflate anion in the metal coordination sphere. Water occupies the apical position and completes the square-pyramidal coordination geometry. Again, metrical data are highly similar to the respective sulfonate complex (Table 1).

Initial reactions with  $\beta$ -alanine instead of anthranilic acid following the same protocol did not provide the desired complex  $(\mathbf{L2})\text{CuCl}$ , but  $(\mathbf{L2H})\text{CuCl}_2$  in appr. 50% yield (Scheme 4, Fig. S1 and S2). Clearly, formal HX elimination is more difficult with alanine. After addition of additional potassium hydroxide base, the reaction cleanly provided  $(\mathbf{L2})\text{CuCl}$ , **6** (Scheme 4). Complex **6** formed a coordination polymer in the solid state, with square-pyramidal coordination around copper and bridging carboxylate in the apical position (Fig. 2, Table 2). Reactions with copper acetate or copper nitrate did not yield the desired products with or without potassium hydroxide. During one attempt, the acetate complex  $(\mathbf{L2})\text{Cu}(\text{OAc})$  was formed, but it crystallized unfortunately as an adduct with copper acetate,  $(\mathbf{L2})\text{Cu}(\text{OAc}) \cdot \text{Cu}(\text{OAc})_2$  (Scheme 4).  $(\mathbf{L2})\text{Cu}(\text{OAc})$  formed an acetate-bridged coordination polymer, the chains of which were crosslinked by carboxylate coordination to the apical position of the copper acetate paddlewheel complex (Fig. S3). The triflate complex  $(\mathbf{L2})\text{Cu}(\text{OTf})$ , **7**, was prepared by anion exchange of the chloride complex (Scheme 4). As the nitrate complex **3**, triflate complex **7** crystallizes as a tetramer with bridging coordination of the carboxylate group. The triflate anion remains coordinated to copper. The higher flexibility of the aliphatic backbone permitted a weak interaction of the copper centre with the bridging carboxylate oxygen (2.7 Å), resulting in a distorted octahedral coordination geometry (Table 2, Fig. 2).

**Table 2.** Geometrical details of the X-ray structures of **6**, (L2H)CuCl<sub>2</sub>, (L2)Cu(OAc)·Cu(OAc)<sub>2</sub> and **7**

	(L2H)CuCl <sub>2</sub>	<b>6</b>	(L2)Cu(OAc)·Cu(OAc) <sub>2</sub>	<b>7</b>
Cu-O <sub>2</sub> CO		1.948(1)	1.953(3)	1.948(9), 1.955(9)
Cu-N(=C)	2.035(2)	1.983(1)	1.996(4)	1.956(12), 1.974(12)
Cu-N <sub>pyridine</sub>	2.031(2)	2.038(1)	1.018(4)	1.993(10), 2.019(10)
Cu-X <sup>a</sup>	2.265(1), 2.274(1)	2.263(1)	1.963(3)	2.268(10), 2.321(10)
Cu-L <sup>a</sup>	2.952(1), 2.570(1)	2.285(1)	2.197(4), 2.616(4)	1.944(9), 1.957(9), 2.672(7), 2.710(10)
τ	0.1	0.1		

<sup>a</sup> (L2H)CuCl<sub>2</sub>: L=μ-Cl<sub>long</sub>, μ-O<sub>2</sub>CR. **6**: X=Cl, L=μ-O<sub>2</sub>CR. (L2)Cu(OAc)·Cu(OAc)<sub>2</sub>: X=OAc, L=μ-OAc, μ-OAc. **7**: X=OTf, L=μ-O<sub>2</sub>CR, μ-O<sub>2</sub>CR.

Reactions of β-alanine with thiophene aldehyde, pyrrole aldehyde or benzaldehyde in the presence of copper(II) chloride did not provide crystalline material. If α-alanine instead of β-alanine was employed, condensation with pyridinecarboxaldehyde in the presence of copper nitrate provided complex **8**, containing a tridentate ligand consisting of one α-alanine and two pyridinecarboxaldehyde moieties (Scheme 5; for its crystal structure, see Fig. S4). Formation of **8** was not investigated in detail, but can be envisioned to proceed via formation of (L)Cu(NO<sub>3</sub>), attack of the C=N double bond on a coordinated pyridinecarboxaldehyde, formal hydrogen shift from methine to N and quarternisation of pyridine by the carbocation. While only a single diastereomer was isolated in 50% of the theoretical yield, the chiral center of alanine reacted under racemization, not inversion. The hydrogen shift from methine to N is thus more likely to proceed via deprotonation-protonation than via a direct 1,2-H shift.

**UV/vis-spectra.** Complexes **1-7** show a d-d transition around 750 nm and an interligand or LMCT transition around 340 nm for **1-5** and around 288 nm for **6** and **7** (Fig. 3). The higher-energy transition is practically invariant with the nature of the anion. The more bathochromic shift in **1-5** can be assigned to the extended π-system of the ligand. The same qualitative trend is observed in iminopyridines with *N*-aryl and *N*-alkyl substituents.<sup>84-85</sup> Only in the acetate complex **4** a somewhat different shape of this transition is observed. A similar trend for the respective sulfonate complexes was explained with persisting bridging coordination of the acetate in solution to form dinuclear (or polynuclear) complexes.<sup>55</sup>

In contrast to the higher-energy transition, the *d-d* transition shows a clear effect of the anion with λ<sub>max</sub> increasing in the order AcO<sup>-</sup> < TfO<sup>-</sup> < Cl<sup>-</sup> = NO<sub>3</sub><sup>-</sup> for **1-5**, as well as for **6**, **7** and

(**L2**)Cu(OAc)·Cu(OAc)<sub>2</sub>. This correlates qualitatively with expectations about the coordinating ability of the anion and is consistent with the anion-displacement equilibria in solution claimed to be present in the sulfonate analogs **B**.<sup>57</sup>

**rac-Lactide polymerization.** Preparation of copper alkoxide complexes (**L1**)Cu(OR) was attempted by reaction of Cu(OMe)<sub>2</sub> or Cu(O*i*Pr)<sub>2</sub> with **L1H** in the best purity available. Reaction in either THF or acetonitrile provided strongly colored solutions, but no crystalline product could be obtained. Alternatively, **2-5** were reacted with NaOMe, NaOEt or KOtBu in various solvents. Again, strong coloration of reaction solutions indicated reactivity, but no product could be isolated. The copper alkoxide complexes required for coordination-insertion polymerization were thus prepared *in situ* by addition of one equiv sodium methoxide to lactide polymerizations with **2-6**. Alternatively, polymerization via an *activated-monomer mechanism* was investigated with one equiv benzyl alcohol as co-initiator. In this mechanism, ring-opening of metal-coordinated lactide is not achieved by intramolecular insertion into a metal-alkoxide bond, but by intermolecular attack of free alcohol to form – after proton transfer – a new, free polymeryl alcohol.

Activities of **2-6** in lactide polymerization are summarized in table 3; full data on all polymerizations can be found in table S1. For ease of comparison, all reactions were quenched after 12 h. Activities determined after 2 h reaction time (Table S1), are in rough agreement with conversions after 12 h, indicating that lack of full conversion is not due to catalyst decomposition. It is important to note that **3-5** contained water in their crystal structures, but that **2** and **6** did not. At room temperature in dichloromethane solution all complexes were inactive towards polymerization either in the absence or presence of either sodium methoxide or benzyl alcohol. Complexes **2**, **3**, **5** and **6** were likewise inactive in toluene at 90 °C, but acetate complex **4** showed a moderate conversion of 40% after 12 h, with a very slight heterotactic preference ( $P_r = 0.60$ ) (Table 3, S1). In the presence of 1 equiv benzyl alcohol, reactivities were identical : **4** produced PLA in 44% conversion after 12 h ( $P_r = 0.63$ ), the others were inactive. With sodium methoxide as co-initiator, **2**, **3** and **5** became active and achieved conversions of 60-95% after 12 h. **6** was not active and, curiously, acetate complex **4** became less active upon addition of sodium methoxide. In melt polymerizations at 140 °C without co-initiator, complexes **2-4** were active (71-96% conversion after 12 h,  $P_r = 0.69-0.84$ ), while **5-7** were not (<25% after 12 h). In the presence of 1 equiv of benzyl alcohol, in general

the same observations were made, although the activity of **4** was reduced and **7** showed 74% conversion. Stereocontrol was similar to reactions without initiator ( $P_r = 0.62-0.85$ ). In the presence of sodium methoxide, melt polymerizations presented a very different picture: All complexes **2-7** were now active with 75-93% conversion after 12 h and the obtained polymers showed notably reduced heterotacticity ( $P_r = 0.52-0.61$ ). Polydispersities ranged from 1.1 to 1.6 (Table S1), without any obvious correlation to reaction conditions or catalyst. All polymerization showed drastically lower than expected polymer molecular weights. The only exception being melt polymerizations in the presence of NaOMe, where polymer molecular weights were notably larger, even if still lower than expected (Table S1).

**Table 3.** Activities of **2-7** in *rac*-lactide polymerization under different conditions. <sup>a</sup>

Conditions	<b>2</b> (Cl)	<b>3</b> (NO <sub>3</sub> )	<b>4</b> (OAc)	<b>5</b> (OTf)	<b>6</b> (Cl)	<b>7</b> (OTf)
RT, CH <sub>2</sub> Cl <sub>2</sub>	n. r.	n. r.	n. r.	n. r.	n. r.	
RT, CH <sub>2</sub> Cl <sub>2</sub> , 1 equiv BnOH	n. r.	n. r.	n. r.	n. r.	n. r.	
RT, CH <sub>2</sub> Cl <sub>2</sub> , 1 equiv NaOMe	n. r.	n. r.	n. r.	n. r.	n. r.	
90 °C, toluene	n. r.	n. r.	40%	n. r.	n. r.	
90 °C, toluene, 1 equiv BnOH	n. r.	n. r.	44%	n. r.	n. r.	
90 °C, toluene, 1 equiv NaOMe	95%	60%	16%	91%	n. r.	
90 °C, toluene, 1 equiv NaOMe + BnOH	20%	12%	10%	15%	n. r.	
140 °C, no solvent	96%	80%	71%	17%	22%	17%
140 °C, no solvent, 1 equiv BnOH	100%	90%	39%	16%	28%	74%
140 °C, no solvent, 1 equiv NaOMe	85%	76%	93%	74%	76%	75%

<sup>a</sup> All reactions were quenched after 12 h. For conversions after 2 h, see table S1. n. r. = no reaction

The ensemble of polymerization results is difficult to interpret mechanistically. Polymerizations at 90 °C agree with a coordination-insertion polymerization catalyzed by copper complexes: In the absence of co-initiator only acetate complex **4** is active, bearing the only anion which could reasonably be expected to initiate polymerization. That activity is unaffected by addition of benzyl alcohol, but increased upon addition of sodium methoxide, likewise supports a coordination-insertion mechanism. One would have expected that water-containing and water-free complexes react differently upon addition of sodium methoxide, but, considering the activity of the acetate complex, catalysts may be able to recover from hydrolysis if the copper hydroxides formed react with lactide to form copper carboxylate salts. Sodium methoxide itself is active under these conditions (Table S1), but unlikely to be the

active species: (a) The microstructure of PLA produced with **2**, **3** and **5** was slightly heterotactic ( $P_r = 0.66 - 0.71$ ), while anionic polymerization with sodium methoxide produces atactic PLA (Table S1). (b) In the presence of **6**, which does not contain water in its crystal structure, no polymer was obtained, indicating that sodium methoxide was not available for polymerization in this case.

The activity of **2-4** in melt polymerizations without co-initiator is puzzling: For an activated-monomer mechanism, water would be the most likely initiator, but water-free **2** was active, while **5**, containing coordinated water, was not. Also, polymerizations in the presence of benzyl alcohol did not show the rate increase which would be expected if initiation by protic impurities is replaced by an added alcohol. In fact, the activity of **4** was reduced by the addition of benzyl alcohol: activities decreased in the order 71%, 62%, and 39% in the presence of 0, 0.2, and 1 equiv of benzyl alcohol, respectively. The effect is not limited to benzyl alcohol: addition of 1 equiv of isopropanol or phenol to polymerizations with **4** likewise reduced activity from 71% to 44% and 40%, respectively (Table S1). Intrigued by this, we repeated polymerizations with **2**, **3** and **5** at 90 °C in the presence of sodium methoxide, but now with an additional equivalent of benzyl alcohol. Activities were again suppressed from 60-95% to 12-20% (Table 3). The fact that suppression of activity occurred with different alcohols and was dependent on the amount of alcohol used, argues against contaminations or decomposition reactions as explanation for the reduced activity. We do not have a mechanistic explanation for the negative impact of additional alcohol on reactivity, but it is clearly incompatible with an activated-monomer mechanism.

While the acetate anion in **4** could be considered a potential initiating group, chloride and nitrate anions are not expected to initiate polymerization by a coordination-insertion mechanism, even at 140 °C. Considering the activity of acetate complex **4** at 90 °C, the ligand carboxylate group is most likely responsible for activity at 140 °C, either by direct insertion into Cu-acyl or by deprotonation of protic impurities. The latter is unlikely, since activity of **2** was unaffected by addition of either water or lactic acid (Table S1), and insertion into the carboxylate group is thus the most likely mechanism (Scheme 6). MALDI-analyses of polymers obtained with **2** and **4** in the presence and absence of benzyl alcohol all show the presence of a series with  $m/z = 72 \cdot n + M(\text{Na})$ , indicative of cyclic oligomers produced by intramolecular transesterification. A second series of  $m/z = 72 \cdot n + 18 + M(\text{Na})$  indicates

hydroxyl-terminated linear chains for **4**, as well as for water-free **2**. The latter probably result from opening of cyclic oligomers by water under MS conditions. For PLA obtained in the presence of benzyl alcohol, a series of benzyl-terminated chains is likewise obtained, which might arise either from benzyl alcohol acting as chain-transfer reagent or from opening of cyclic oligomers by reaction with benzyl alcohol under MS conditions. It is tempting to assign the high amount of intramolecular transesterification to the formation of a reactive carbonate group at the chain end, close to the metal alkoxide (Scheme 6). The latter would encourage formation of cyclic oligomers, in a mechanism similar to that proposed for NHC-catalyzed polymerization of lactide.<sup>86</sup> However, the low polymer molecular weights were also observed for polymerizations at 90 °C, in complexes which were active only in the presence of sodium methoxide.

For melt polymerization in the presence of sodium methoxide, similar activities of all catalysts, reduced heterotacticity of the polymer and increased polymer molecular weights, all indicate that sodium methoxide does not react (completely) with LCuX under these conditions and is at least partly responsible for the formation of polymer produced at 140 °C.

Complexes **6** and **7** with an aliphatic backbone display – on average – lower activities (Table 3, S1). Taken aside the activity of the acetate complex at 90 °C, there is no clear correlation of activity with the nature of the anion.  $P_r$  values vary strongly under similar conditions without any correlation to the nature of the anion, indicative that **2-7** do not reliably form a single active species under these conditions.

**Chan-Evans-Lam couplings.** A drawback of typical CEL couplings with simple copper salts is the high substrate dependence on reaction conditions, which in most cases require the optimization of reaction conditions even for closely related substrates, such as aniline and amine.<sup>87-88</sup> Complexes **B** were shown to be not just highly reactive in CEL couplings, but also to function with a simple and general reaction protocol (various solvents tolerated, water tolerated, no base or ligand additive required, and applicable for aniline, amines as well as other *N*-nucleophiles under identical conditions).<sup>55-57</sup> This was rationalized by the fact that the ligand is responsible for solubilisation of the complex and – via the sulfonate group in **B** – coordinates to boron to form a dinuclear complex, proposed as an intermediate prior to transmetallation.<sup>89-91</sup> In CEL couplings with simple copper salts, the anion typically acts as the bridging ligand. Consequently, CEL couplings with CuX<sub>2</sub> salts normally show a strong

dependence of activity on the counteranion, while couplings with **B** did not. Complexes **1-7** were investigated in CEL couplings to see if these characteristics can be transferred to a carboxylate-based ligand or if the sulfonate group is essential. Complexes **1-7** were active in CEL couplings under the exact same reaction conditions employed for **B**, i. e. room temperature, methanol solution, 1.5 equiv PhB(OH)<sub>2</sub>, 2.5 mol% catalyst, no base or further ligand added (Scheme 7).

As for **B**, neither deboration, nor coupling to solvent, nor aryl homocoupling was observed. An excess phenylboronic acid is thus not necessary to for the reactions to reach completion, but was employed to allow comparison with data for **B**. Full conversion was reached for the coupling of the more nucleophilic cyclohexylamine and *n*-octylamine with phenylboronic acid using **1-5** (Table 4). For aniline as nucleophile, however, using chloride and triflate complexes **1** and **5** did not lead to full conversion (Table 4). The reason for this is unclear and does not correlate with qualitative coordination strength of the anions to copper. Reactions with cyclohexylamine were investigated in detail to address the dependence of reactivity on the counteranion. In the mechanism proposed for **B**, the reactive species is proposed to be cationic and the anion involvement is limited to its influence on the dissociation equilibrium. Consequently, only a small influence of the anion on reactivity was observed for complexes **B**.<sup>55</sup> The same was observed for **1-5**: apparent first-order rate constants varied by less than a factor of two between the most and the least active complex (Fig. 4, Table 4). The anion has, however a remarkable influence on the length of the induction period, which differed between 5 – 70 min. As expected, the more nucleophilic substrates cyclohexylamine and *n*-octylamine show 4-5 times higher reactivity than aniline (Table 4).

**Table 4.** Chan-Evans-Lam coupling with phenylboronic acid

Catalyst	Anion	Aniline	<i>n</i> -Octylamine	Cyclohexylamine		
		Conversion <sup>a</sup>	Conversion <sup>b</sup>	Conversion <sup>a</sup>	$k_{\text{obs}}$	$t_0$
<b>1</b>	Cl <sup>-</sup>	25%	100%	95%	0.39(1) h <sup>-1</sup>	5 min
<b>3</b>	NO <sub>3</sub> <sup>-</sup>	100%	100%	100%	0.34(2) h <sup>-1</sup>	70 min
<b>4</b>	AcO <sup>-</sup>	100% <sup>c</sup>	100% <sup>d</sup>	100%	0.67(1) h <sup>-1</sup>	20 min
<b>5</b>	TfO <sup>-</sup>	26%	100%	96%	0.48(5) h <sup>-1</sup>	45 min
<b>6</b>	Cl <sup>-</sup>	23%	100%	48%	> 0.3 h <sup>-1</sup>	>210 min
<b>7</b>	TfO <sup>-</sup>	0%	100%	80%	> 0.09 h <sup>-1</sup>	330 min
<b>8</b>	NO <sub>3</sub> <sup>-</sup>	0%	100%	100%	0.19(4) h <sup>-1</sup>	120 min

<sup>a</sup> after 12 h. <sup>b</sup> after 4.5 h. <sup>c</sup>  $k_{\text{obs}} = 0.13(4) \text{ h}^{-1}$  <sup>d</sup>  $k_{\text{obs}} = 0.51(4) \text{ h}^{-1}$

While still highly competent in CEL couplings, replacing the sulfonate group with a carboxylate in **1-5** resulted in an overall drop of activity compared to complexes of type **B** (Scheme 1). Coupling with aniline was appr. 4-5 times faster with **B** and reactions with octylamine which require several hours with **1-5** reach completion in 10 min with **B**. The lower reactivity might be associated with the geometry of the carboxylate vs. the sulfonate group: Coordination of boron to the rigid carboxylate group places the phenylboronic acid by necessity farther away from the copper center than coordination to the tetrahedral and more flexible sulfonate group (Scheme 8).

Couplings with **6** and **7**, having an alkyl backbone in the ligand, show smaller rate constants and significantly longer induction periods. As for **B**, dissociation of the anionic ligand from copper thus seems not to be required in the catalytic cycle. Complex **8** shows, despite the complex nature of the ligand backbone, the same general characteristics as **1-7**, i. e. a tridentate, mono-anionic ligand with a coordinated carboxylate. As such, it was likewise tested in CEL couplings and proved to be a competent catalyst under the same mild reaction conditions for amines, but not for aniline (Table 4).

**Substrate scope in comparison to sulfonate complexes B.** Complexes of type **B** were not reactive toward weaker nucleophiles, such as alcohols or phenols. They also did not show any reactivity with alkylboronic acids. Complexes **1-5** unfortunately showed the same lack of reactivity. Neither coupling of phenol or alcohol with phenylboronic acid, nor coupling of octylamine or aniline with *sec*-butylboronic acid or cyclohexylboronic acid was observed under a variety of reaction conditions and up to temperatures of 120 °C.

## Conclusions

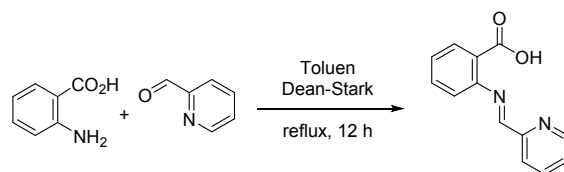
Pyridylimino carboxylate copper(II) complexes based on anthranilic acid or  $\beta$ -alanine with different anions are readily available from simple starting materials in a one-pot reaction. While copper(II) alkoxide complexes could not be isolated, *rac*-lactide polymerization data supports a coordination-insertion mechanism by copper alkoxide complexes under some conditions. This is in contrast to polymerization with their sulfonate analogs and replacement of sulfonate by carboxylate thus indeed increased the accessibility of copper(II) alkoxide complexes. Several mechanisms seem to be in play, however, and at 140 °C sodium methoxide seems to initiate polymerization on its own instead of reacting with the copper complexes. Although a step up from the performance of their sulfonate analogs, catalyst performance remains highly unsatisfactory with low and irregular activities, moderate heterotacticities, and severe lack of polymer molecular weight control. Compared to our previous work which showed excellent stereocontrol with Cu(II) complexes, the lack of steric bulk towards the apical positions of the copper complex might be responsible for the lack of polymer molecular weight control.

In CEL couplings, in particular anthranilic acid-based complexes **1-5** were competent catalysts. There is no evidence of typically observed side reactions, such as deboration or aryl homocoupling, and they are active for amines as well as anilines under the same, unoptimized reaction conditions. While they still outperform the simple copper salts typically employed, their performance is somewhat lower than that of the corresponding sulfonate complexes recently reported by our group. This can gratifyingly be explained by the structure of the carboxylate- or sulfonate-bridged dinuclear copper-boron species proposed in the mechanism for these complexes. Catalyst design for CEL couplings should thus include groups able to coordinate to boron which either place the boronic acid in close contact to the metal center or contain sufficient intermolecular flexibility to allow it to approach the copper center in the transmetallation step.

## Experimental section

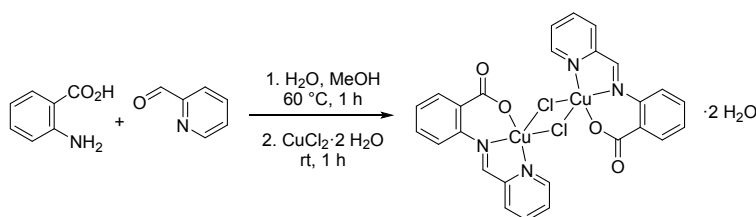
**General.** Phenylboronic acid was purified by washing with dichloromethane until the filtrate stayed colorless. *rac*-Lactide (98%) was purchased from Sigma–Aldrich, purified by 3 recrystallizations from dry ethyl acetate and kept at –30 °C. All other chemicals were purchased from common commercial suppliers and used without further purification. Elemental analyses were performed by the Laboratoire d'analyse élémentaire (Université de

Montreal). UV/vis spectra were recorded on a Cary Series UV-Vis-NIR spectrophotometer from Agilent Technology. GC-MS spectra were recorded on an Agilent Technology GC/MS.



**2-((Pyridin-2-ylmethylene)amino)benzoic acid, L1H.** 2-Pyridinecarboxaldehyde (95  $\mu\text{L}$ , 1.0 mmol) and aniline-2-carboxylic acid (anthranilic acid, 137 mg, 1.0 mmol) were dissolved in anhydrous toluene (15 mL). The mixture was refluxed overnight, cooled to room temperature and filtered. After evaporation of the solvent, the residue was analyzed by  $^1\text{H}$  NMR to show 80% conversion to product. Purification by column chromatography with a gradient of solvent from 8/2 : hexane/ethyl acetate to 2/8 : hexane/ethylacetate yielded the product in 95% purity according to NMR (147 mg, 65%).

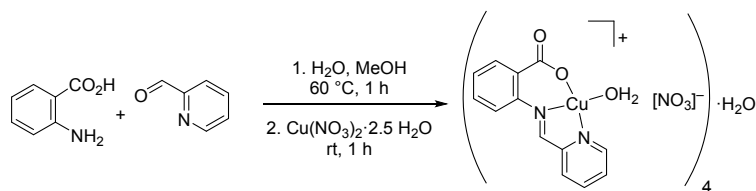
$^1\text{H}$  NMR (DMSO- $d_6$ , 400 MHz)  $\delta\text{H}$ : 8.66 (d,  $J = 4$ , 1H, py), 8.00 (s, 1H, PyCH(=N)), 7.74 (t,  $J = 8$ , 1H, Py), 7.5 (m, 2H), 7.2 (m, 2H), 7.05 (d,  $J = 8$ , 1H), 6.90 (t,  $J = 8$ , 1H), 6.31 (s, 1H CO<sub>2</sub>H). Anal. Calcd. for C<sub>13</sub>H<sub>10</sub>N<sub>2</sub>O<sub>2</sub>: C, 69.02; H, 4.46; N, 12.38. Found: C, 69.43; H, 4.78; N, 12.02. HRMS(ESI),  $m/z$  (M+H<sup>+</sup>, 100), Calcd. for C<sub>13</sub>H<sub>11</sub>N<sub>2</sub>O<sub>2</sub>: 227.0826, Found: 227.0815.



**(L1)<sub>2</sub>Cu<sub>2</sub>( $\mu$ -Cl)<sub>2</sub> · 2 H<sub>2</sub>O, 1.** 2-Pyridinecarboxaldehyde (95  $\mu\text{L}$ , 1.0 mmol) was added to a hot solution (60 °C) of aniline-2-carboxylic acid (anthranilic acid, 137 mg, 1.0 mmol) in water/methanol (5/10 mL). The mixture was stirred for one hour at 60 °C. CuCl<sub>2</sub> · 2 H<sub>2</sub>O (187 mg, 1.1 mmol) was added, heating was stopped and the green solution was stirred another hour. After filtration, slow evaporation of the solvent afforded green, X-ray quality crystals (256 mg, 75%).

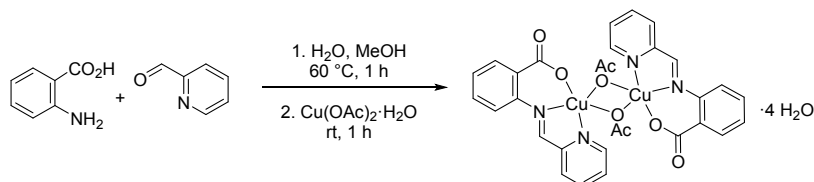
UV-vis (DMSO, 4.0 · 10<sup>-3</sup> M or 6.17 · 10<sup>-5</sup> M) [ $\lambda_{\text{max}}$ , nm ( $\epsilon$ , M<sup>-1</sup> · cm<sup>-1</sup>): 338 (9132), 719 (40). Anal. Calcd. for C<sub>13</sub>H<sub>9</sub>ClCuN<sub>2</sub>O<sub>2</sub> · 1 H<sub>2</sub>O: C, 45.62; H, 3.24; N, 8.19. Found: C, 45.35; H, 3.15; N, 8.00.

**{(L1)Cu( $\mu$ -Cl)}<sub>2</sub> · 2 MeOH, 2.** Recrystallisation of **1** (100 mg, 0.29 mmol) in anhydrous MeOH (2 mL) led to copper complexes with a co-crystallized methanol (35 mg, 34%). UV-vis (DMSO, 4.8 · 10<sup>-3</sup> M or 6.2 · 10<sup>-5</sup> M) [ $\lambda_{\text{max}}$ , nm ( $\epsilon$ , M<sup>-1</sup> · cm<sup>-1</sup>): 338 (9196), 719 (51). Anal. Calcd. for C<sub>13</sub>H<sub>9</sub>ClCuN<sub>2</sub>O<sub>2</sub> · MeOH: C, 47.20; H, 3.68; N, 7.86. Found: C, 46.88; H, 3.34; N, 7.49.



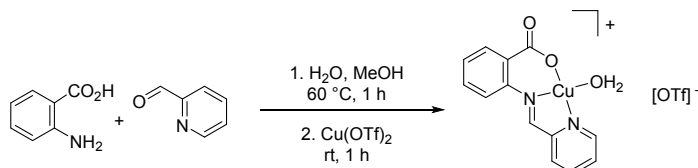
$[(\mathbf{L1})\text{Cu}(\text{OH}_2)]_4[\text{NO}_3]_4$ , **3**. Equivalent to **1**, from  $\text{Cu}(\text{NO}_3)_2 \cdot 2.5 \text{H}_2\text{O}$  (255 mg, 1.1 mmol). Slow evaporation of the solvent provided green, X-ray quality crystals (306 mg, 83%).

UV-vis (DMSO,  $4.5 \cdot 10^{-3} \text{ M}$  or  $5.6 \cdot 10^{-5} \text{ M}$ ) [ $\lambda_{\text{max}}$ , nm ( $\epsilon$ ,  $\text{M}^{-1}\text{cm}^{-1}$ ): 338 (8041), 717 (47)]. Anal. Calcd. for  $\text{C}_{13}\text{H}_9\text{CuN}_3\text{O}_5 \cdot 1\frac{1}{4}\text{H}_2\text{O}$ : C, 41.83; H, 3.10; N, 11.26. Found: C, 42.01; H, 3.18; N, 11.11.



$(\mathbf{L1})_2\text{Cu}_2(\mu\text{-OAc})_2 \cdot 4 \text{H}_2\text{O}$ , **4**. Equivalent to **1**, from  $\text{Cu}(\text{OAc})_2 \cdot \text{H}_2\text{O}$  (219 mg, 1.1 mmol). Slow evaporation of the solvent yielded green, X-ray quality crystals (222 mg, 58%).

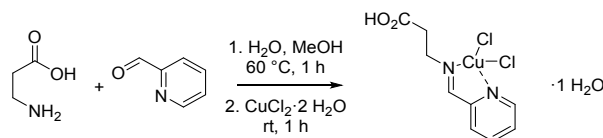
UV-vis (DMSO,  $4.6 \cdot 10^{-3} \text{ M}$  or  $4.0 \cdot 10^{-5} \text{ M}$ ) [ $\lambda_{\text{max}}$ , nm ( $\epsilon$ ,  $\text{M}^{-1}\text{cm}^{-1}$ ): 327 (6871), 690 (86)]. Anal. Calcd. for  $\text{C}_{15}\text{H}_{12}\text{CuN}_2\text{O}_4 \cdot 2 \text{H}_2\text{O}$ : C, 46.94; H, 4.20; N, 7.30. Found: C, 46.36; H, 4.33; N, 7.64.



$\{[(\mathbf{L1})\text{Cu}(\text{OH}_2)]\}_n[\text{OTf}]$ , **5**. **Method 1**: Equivalent to **1**, from  $\text{Cu}(\text{OTf})_2$  (398 mg, 1.1 mmol). Slow evaporation of the solvent provided green, X-ray quality crystals (332 mg, 73%).

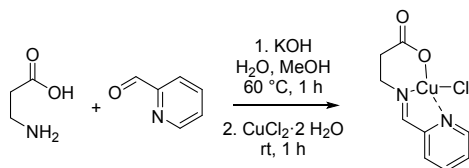
UV-vis (DMSO,  $3.9 \cdot 10^{-3} \text{ M}$  or  $4.9 \cdot 10^{-5} \text{ M}$ ) [ $\lambda_{\text{max}}$ , nm ( $\epsilon$ ,  $\text{M}^{-1}\text{cm}^{-1}$ ): 338 (8470), 697 (65)]. Anal. Calcd. for  $\text{C}_{14}\text{H}_9\text{CuF}_3\text{N}_2\text{O}_5\text{S}_1 \cdot 1.5 \text{H}_2\text{O}$ : C, 36.17; H, 2.60; N, 6.03; S, 6.90. Found: C, 36.26; H, 2.77; N, 6.37; S, 7.23.

**Method 2**: Silver triflate (75 mg, 0.40 mmol) was added to a suspension of **1** (100 mg, 0.29 mmol) in dry THF (10 mL) under nitrogen. After one hour of stirring at ambient temperature, a precipitate appeared and the color of the solution intensified. After filtration, slow evaporation of the green solution (under  $\text{N}_2$ ), afforded green crystals (83 mg, 63%). The compound shows the same crystal structure and an identical UV/vis spectrum to the one prepared above.



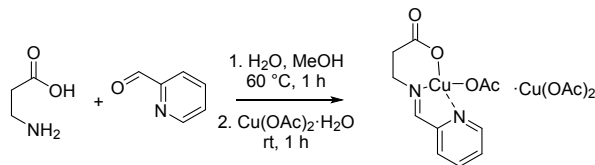
**(L2H)CuCl<sub>2</sub>·H<sub>2</sub>O**. Equivalent to **1**, from  $\beta$ -alanine (89 mg, 1.0 mmol), 2-pyridinecarboxaldehyde (95  $\mu$ L, 1.0 mmol) and  $\text{CuCl}_2 \cdot 2 \text{H}_2\text{O}$  (187 mg, 1.1 mmol). Slow evaporation of the solvent yielded green, X-ray quality crystals (171 mg, 49%).

UV-vis (DMSO,  $5.1 \cdot 10^{-3}$  M or  $6.4 \cdot 10^{-5}$  M) [ $\lambda_{\text{max}}$ , nm ( $\epsilon$ ,  $\text{M}^{-1} \cdot \text{cm}^{-1}$ )]: 288 (7442), 741 (95). Anal. Calcd. for  $\text{C}_9\text{H}_{10}\text{CuN}_2\text{O}_2\text{Cl}_2 \cdot 1 \text{H}_2\text{O}$ : C, 32.69; H, 3.66; N, 8.47. Found: C, 32.34; H, 3.68; N, 8.11.



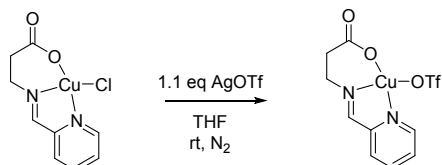
**(L2)<sub>2</sub>Cu<sub>2</sub>( $\mu$ -Cl)<sub>2</sub>·6**. 2-Pyridinecarboxaldehyde (95  $\mu$ L, 1.0 mmol) and potassium hydroxide (56 mg, 1.0 mmol) were added to a hot solution (60 °C) of 3-propanoic acid ( $\beta$ -alanine, 89 mg, 1.0 mmol) in water/methanol (5/10 mL). The mixture was stirred for one hour at 60 °C.  $\text{CuCl}_2 \cdot 2 \text{H}_2\text{O}$  (187 mg, 1.1 mmol) was added, heating was stopped and the solution was stirred another hour. After filtration, slow evaporation of the solvent afforded blue-green, X-ray quality crystals (214 mg, 78%).

UV-vis (DMSO,  $6.1 \cdot 10^{-3}$  M or  $7.6 \cdot 10^{-5}$  M) [ $\lambda_{\text{max}}$ , nm ( $\epsilon$ ,  $\text{M}^{-1} \cdot \text{cm}^{-1}$ )]: 288 (5794), 786 (62). Anal. Calcd. for  $\text{C}_9\text{H}_9\text{ClCuN}_2\text{O}_2$ : C, 39.14 H, 3.28; N, 10.14. Found: C, 38.80 H, 3.53; N, 9.78.



**(L2)Cu(OAc)·Cu(OAc)<sub>2</sub>**. Equivalent to **1**, from 3-aminopropanoic acid ( $\beta$ -alanine, 89 mg, 1.0 mmol), 2-pyridinecarboxaldehyde (95  $\mu$ L, 1.0 mmol), and  $\text{Cu(OAc)}_2 \cdot \text{H}_2\text{O}$  (219 mg, 1.1 mmol). Slow evaporation of the solvent yielded blue-green, X-ray quality crystals (216 mg, 45%).

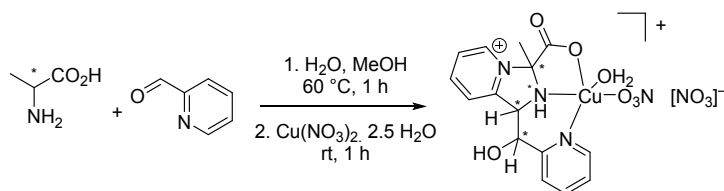
UV-vis (DMSO,  $0.6 \cdot 10^{-2}$  M or  $33 \cdot 10^{-4}$  M) [ $\lambda_{\text{max}}$ , nm ( $\epsilon$ ,  $\text{M}^{-1} \cdot \text{cm}^{-1}$ )]: 305 (2500), 716 (115). Anal. Calcd. for  $\text{C}_{11}\text{H}_{12}\text{CuN}_2\text{O}_4 \cdot \text{Cu(OAc)}_2$ : C, 37.42; H, 3.77; N, 5.82. Found: C, 37.76; H, 4.01; N, 6.49.



**(L2)CuOTf·6**. Silver triflate (104 mg, 0.40 mmol) was added to a suspension of **1** (100 mg, 0.37 mmol) in dry THF (10 mL) under nitrogen atmosphere. After one hour of reaction at ambient temperature, a precipitate appeared

and the color of the solution intensified. After filtration, slow evaporation of the green solution (under  $N_2$ ), afforded green crystals (95 mg, 66%).

UV-vis (DMSO,  $2.7 \cdot 10^{-2}$  M or  $1.3 \cdot 10^{-4}$  M) [ $\lambda_{max}$ , nm ( $\epsilon$ ,  $M^{-1} \cdot cm^{-1}$ ): 285 (4230), 703 (32). Anal. Calcd. for  $C_{10}H_9CuF_3N_2O_5S_1$ : C, 30.81; H, 2.33; N, 7.19 S, 8.22. Found: C, 30.49; H, 2.64; N, 6.85; S, 8.76.



$[(L3)Cu(H_2O)(NO_3)][NO_3]$ , **8**. Equivalent to **1**, from (*S*)-2-aminopropanoic acid (L-alanine, 89 mg, 1.0 mmol), 2-pyridinecarboxaldehyde (95  $\mu$ L, 1.0 mmol) and  $Cu(NO_3)_2 \cdot 2.5 H_2O$  (255 mg, 1.1 mmol). Slow evaporation of the solvent yielded green, X-ray quality crystals (50 mg, 25%).

UV-vis (DMSO,  $1.0 \cdot 10^{-2}$  M or  $1.0 \cdot 10^{-4}$  M) [ $\lambda_{max}$ , nm ( $\epsilon$ ,  $M^{-1} \cdot cm^{-1}$ ): 259 (8046), 826 (32).

### ***rac*-Lactide polymerization**

**At room temperature or 90 °C:** Under nitrogen, the catalyst (0.01 mmol) was added to lactide (144 mg, 1.0 mmol) in dry dichloromethane (1 mL) or dry toluene (1 mL). If desired, benzyl alcohol ( $5.0 \times 10^{-2}$  M in  $CH_2Cl_2$ ) and/or a stock solution of sodium methoxide ( $5.0 \times 10^{-2}$  M in  $CH_2Cl_2$ ) was added to the reaction mixture. For reactions at 90 °C, the reactions vessel was sealed and placed in a pre-heated oil-bath. Reaction mixtures were quenched at the desired polymerization time by addition of a dichloromethane solution of acetic acid (5 mM). Dry polymer samples were stored at  $-80$  °C.

**At 140 °C :** In a pressure tube under nitrogen, the catalyst (0.010 mmol) was combined with lactide (144 mg, 1.0 mmol). If desired, benzyl alcohol ( $5.0 \times 10^{-2}$  M in  $CH_2Cl_2$ ) and/or a stock solution of sodium methoxide ( $5.0 \times 10^{-2}$  M in  $CH_2Cl_2$ ) was added to the reaction mixture. The tube was placed in a pre-heated oil bath outside the glovebox. Reaction mixtures were quenched at the desired polymerization time by addition of a dichloromethane solution of acetic acid (5 mM), rapidly cooled to RT and the solvent evaporated. Dry polymer samples were stored at  $-80$  °C.

**Characterization.** Conversion was determined from  $^1H$  NMR by comparison to remaining lactide.  $P_r$  values were determined from homodecoupled  $^1H$  NMR spectra and calculated from  $P_r = 2 \cdot I_1 / (I_1 + I_2)$ , with  $I_1 = 5.15 - 5.21$  ppm (*rmr*, *mmr/rmm*),  $I_2 = 5.21 - 5.25$  ppm (*mmr/rmm*, *mmm*, *mrm*). The integration of the left multiplet and right multiplet ( $I_1$  and  $I_2$ ) required only one, very reproducible dividing point of the integration, which was always taken as the minimum between the two multiplets.  $P_r$ -values obtained this way were typically consistent to  $\pm 1\%$  over the course of one experiment and  $\pm 3\%$  between different experiments under identical conditions. Molecular weight analyses were performed on a Waters 1525 gel permeation chromatograph equipped with three Phenomenex columns and a refractive index detector at 35 °C. THF was used as the eluent at a flow rate of  $1.0 mL \cdot min^{-1}$  and

polystyrene standards (Sigma–Aldrich, 1.5 mg mL<sup>-1</sup>, prepared and filtered (0.2 mm) directly prior to injection) were used for calibration. Obtained molecular weights were corrected by a Mark-Houwink factor of 0.58.<sup>92</sup>

**General procedure for Chan-Evans-Lam couplings.** To a solution of amine (1.0 mmol) and phenylboronic acid (1.5 mmol) in methanol (1 mL) was added the desired catalyst (0.025 mmol). Trimethoxybenzene was added as internal standard. The reaction was stirred open to air at ambient temperature. For kinetic experiments, 20 µL aliquots were taken, diluted in ethyl acetate and analyzed by GC-MS. After the desired reaction time, the reaction was quenched with 0.5 mL of a saturated aqueous solution of ammonium chloride. The organic layer was extracted and filtered through a short silica plug to remove remaining copper complex. Products and side-products were identified in the MS- and NMR-spectra from comparison to literature. Conversion was typically analysed by GC-MS. Quantitative concentrations were determined by comparison to trimethoxybenzene standard. Calibration factors between starting materials, products, side-products and trimethoxybenzene were determined from simultaneous NMR and GC-MS analysis or by analysis of solutions prepared from isolated or commercially available products.

**X-ray diffraction studies.** Crystal for X-ray diffraction were obtained from synthesis as described above. Diffraction data were collected on a Bruker Venture METALJET diffractometer (Ga K $\alpha$  radiation) or a Bruker APEX II microsource (Cu K $\alpha$  radiation).<sup>93</sup> Data reduction was performed with SAINT,<sup>94</sup> absorption corrections with SADABS.<sup>95</sup> Structures were solved by dual-space refinement (SHELXT).<sup>96</sup> All non-hydrogen atoms were refined anisotropic using full-matrix least-squares on  $F^2$  and hydrogen atoms refined with fixed isotropic U using a riding model (SHELXL97).<sup>97</sup> Complexes **2**, **3**, and **7** suffered from mediocre to bad crystal quality, but the obtained structural data is sufficient to uphold the conclusions in the main text. Further experimental details can be found in Table 5 and the supporting information (CIF).

**Table 5.** Details of X-ray Diffraction Studies

	<b>1</b>	<b>2</b>	<b>3</b>	<b>4</b>	<b>5</b>
Formula	C <sub>26</sub> H <sub>20</sub> Cl <sub>2</sub> Cu <sub>2</sub> N <sub>4</sub> O <sub>5</sub>	C <sub>27</sub> H <sub>22</sub> Cl <sub>2</sub> Cu <sub>2</sub> N <sub>4</sub> O <sub>5</sub>	C <sub>52</sub> H <sub>46</sub> Cu <sub>4</sub> N <sub>12</sub> O <sub>25</sub>	C <sub>15</sub> H <sub>16</sub> CuN <sub>2</sub> O <sub>6</sub>	C <sub>14</sub> H <sub>11</sub> CuF <sub>3</sub> N <sub>2</sub> O <sub>6</sub> S
$M_w$ (g/mol); F(000)	666.44; 672	680.46; 688	1493.17; 6064	383.84; 1576	455.85; 3664
$T$ (K); wavelength	150; 1.34190	150; 1.34190	150; 1.34190	150; 1.34190	150; 1.34190
Crystal System	Triclinic	Triclinic	Monoclinic	Orthorhombic	Orthorhombic
Space Group	$P1$	$P1$	$P2_1/c$	$Pbca$	$Fdd2$
Unit Cell: $a$ (Å)	7.0643(2)	9.7464(5)	21.2716(10)	8.5717(2)	22.214(3)
$b$ (Å)	12.7769(4)	11.4104(6)	21.2719(11)	18.0801(5)	37.308(5)
$c$ (Å)	13.9680(4)	13.1040(7)	27.1790(13)	20.4049(6)	7.8781(10)
$\alpha$ (°)	79.5330(10)	107.274(2)	90	90	90
$\beta$ (°)	88.2270(10)	102.216(2)	107.558(3)	90	90
$\gamma$ (°)	80.2220(10)	102.993(3)	90	90	90
$V$ (Å <sup>3</sup> )	1221.76(6)	1293.84(12)	11725.2(10)	3162.29(15)	6529.1(14)
$Z$ ; $d_{\text{calcd.}}$ (g/cm <sup>3</sup> )	2; 1.812	2; 1.747	8; 1.692	8; 1.612	16; 1.855
$\mu$ (mm <sup>-1</sup> ); Abs. Corr.	11.003; multi-scan	10.399; multi-scan	8.286; multi-scan	7.670; multi-scan	8.443; multi-scan
$\theta$ range (°); completeness	2.8-53.6; 1.00	3.2-52.3; 1.00	2.6-53.6; 1.00	3.8-53.6; 1.00	4.0-53.6; 0.99
Collected reflections; $R_{\sigma}$	47509; 0.021	55375; 0.051	81161; 0.044	31791; 0.024	20965; 0.049
Unique reflections; $R_{\text{int}}$	5615; 0.042	4614; 0.098	13461; 0.067	3636; 0.046	3504; 0.059
Observed Reflections; $R1(F)$	5502; 0.031	3491; 0.113	12030; 0.095	3091; 0.075	3226; 0.039
$wR(F^2)$ (all data); GoF( $F^2$ )	0.083; 1.08	0.342; 1.43	0.257; 1.07	0.080; 1.03	0.092; 1.10
Residual electron density	0.67	2.43	3.25	0.39	0.44

Table 5. continued

	6	7	8	(L1H)CuCl <sub>2</sub>	(L1)CuOAc·Cu(OAc) <sub>2</sub>
Formula	C <sub>9</sub> H <sub>9</sub> ClCuN <sub>2</sub> O <sub>2</sub>	C <sub>20</sub> H <sub>18</sub> Cu <sub>2</sub> F <sub>6</sub> N <sub>4</sub> O <sub>10</sub> S <sub>2</sub>	C <sub>15</sub> H <sub>17</sub> CuN <sub>5</sub> O <sub>10</sub>	C <sub>9</sub> H <sub>12</sub> Cl <sub>2</sub> CuN <sub>2</sub> O <sub>3</sub>	C <sub>15</sub> H <sub>18</sub> Cu <sub>2</sub> N <sub>2</sub> O <sub>8</sub>
$M_w$ (g/mol); F(000)	276.17; 1916	779.58; 3120	490.5; 2008	330.65; 668	481.41; 956
$T$ (K); wavelength	100; 1.54178	150; 1.34190	100; 1.54178	100; 1.54178	150; 1.34190
Crystal System	Monoclinic	Monoclinic	Monoclinic	Monoclinic	Monoclinic
Space Group	$P2_1/c$	$P2_1/c$	$P2_1/c$	$P2_1/n$	$P2_1/c$
Unit Cell: $a$ (Å)	7.7942(2)	27.7325(18)	12.4500(2)	8.8166(3)	8.5605(3)
$b$ (Å)	9.8050(3)	7.5286(5)	9.6183(2)	14.6490(5)	26.0642(10)
$c$ (Å)	13.5262(4)	29.643(2)	30.7146(5)	10.1051(3)	8.4229(3)
$\alpha$ (°)	90	90	90	90	90
$\beta$ (°)	104.405(1)	114.689(4)	98.6150(10)	111.372(1)	97.167(2)
$\gamma$ (°)	90	90	90	90	90
$V$ (Å <sup>3</sup> )	1001.20(5)	5623.3(7)	3636.51(11)	1215.37(7)	1864.66(12)
$Z$ ; $d_{\text{calcd.}}$ (g/cm <sup>3</sup> )	4; 1.832	8; 1.842	8; 1.793	4; 1.807	4; 1.296
$\mu$ (mm <sup>-1</sup> ); Abs. Corr.	5.385; multi-scan	9.685; multi-scan	2.362; multi-scan	6.591; multi-scan	12.606; multi-scan
$\theta$ range (°); completeness	5.6-67.7; 0.99	2.9-57.4; 0.99	2.9-67.7; 1.00	5.6-72.1; 0.99	3.0-60.8; 0.99
Collected reflections; $R_{\sigma}$	25743; 0.0099	22199; 0.167	36614; 0.012	29979; 0.012	22025; 0.050
Unique reflections; $R_{\text{int}}$	1937; 0.026	5706; 0.160	3573; 0.026	2356; 0.028	4260 0.072
Observed Reflections; $R1(F)$	1915; 0.024	3088; 0.159	3570; 0.035	2332; 0.024	3408; 0.059
$wR(F^2)$ (all data); GoF( $F^2$ )	0.065; 1.04	0.422; 1.05	0.089; 1.23	0.062; 1.10	0.172; 1.05
Residual electron density	0.53	1.92	0.43	0.65	1.30

## Supporting Information

Figures for crystal structures of (L2H)CuCl<sub>2</sub>, (L2)Cu(OAc)·Cu(OAc)<sub>2</sub> and **8**. Full listings of polymerization experiments. Crystal structure data (CIF).

## Acknowledgements

Funding was supplied by the NSERC discovery program (RGPIN-2016-04953) and the Centre for Green Chemistry and Catalysis (FQRNT). We thank Dr. Thierry Maris for support with X-ray diffraction, Elena Nadezhina for elemental analysis, and Prof. D. Zargarian for access to GC/MS.

## References

- (1) Evano, G.; Blanchard, N., *Copper-Mediated Cross-Coupling Reactions*. John Wiley & Sons: New York, 2013.
- (2) Simon, W. *Angew. Chem., Int. Ed.* **2005**, *44*, 5560-5562.
- (3) Matyjaszewski, K. In *Controlled Radical Polymerization: Mechanisms*, American Chemical Society: 2015; Vol. 1187, pp 1-17.
- (4) Matyjaszewski, K. *Isr. J. Chem.* **2012**, *52*, 206-220.
- (5) Stibrany, R. S., D.; Kacker, S.; Patil, A. (Exxon Research and Engineering) WO 99/30822, 1999.
- (6) Gibson, V. C.; Tomov, A.; Wass, D. F.; White, A. J. P.; Williams, D. J. *J. Chem. Soc., Dalton Trans.* **2002**, 2261-2262.
- (7) Stibrany, R. T.; Schulz, D. N.; Kacker, S.; Patil, A. O.; Baugh, L. S.; Rucker, S. P.; Zushma, S.; Berluce, E.; Sissano, J. A. *Macromolecules* **2003**, *36*, 8584.
- (8) Nagel, M.; Paxton, W. F.; Sen, A.; Zakharov, L.; Rheingold, A. L. *Macromolecules* **2004**, *37*, 9305-9307.
- (9) Olson, J. A.; Boyd, R.; Quail, J. W.; Foley, S. R. *Organometallics* **2008**, *27*, 5333-5338.
- (10) Ikariya, T.; Yamamoto, A. *J. Organomet. Chem.* **1974**, *72*, 145-151.
- (11) Schaper, F.; Foley, S. R.; Jordan, R. F. *J. Am. Chem. Soc.* **2004**, *126*, 2114-2124.
- (12) Le Roux, E. *Coord. Chem. Rev.* **2016**, *306*, 65-85.
- (13) Paul, S.; Zhu, Y.; Romain, C.; Brooks, R.; Saini, P. K.; Williams, C. K. *Chem. Commun. (Cambridge, U. K.)* **2015**, *51*, 6459-6479.
- (14) MacDonald, J. P.; Shaver, M. P. In *Green Polymer Chemistry: Biobased Materials and Biocatalysis*, American Chemical Society: 2015; Vol. 1192, pp 147-167.
- (15) Guillaume, S. M.; Kirillov, E.; Sarazin, Y.; Carpentier, J.-F. *Chem.-Eur. J.* **2015**, *21*, 7988-8003.
- (16) Sauer, A.; Kapelski, A.; Fliedel, C.; Dagorne, S.; Kol, M.; Okuda, J. *Dalton Trans.* **2013**, *42*, 9007-9023.
- (17) Dagorne, S.; Normand, M.; Kirillov, E.; Carpentier, J.-F. *Coord. Chem. Rev.* **2013**, *257*, 1869-1886.
- (18) Dagorne, S.; Fliedel, C. In *Modern Organoaluminum Reagents: Preparation, Structure, Reactivity and Use*, Woodward, S.; Dagorne, S., Eds. Springer Berlin Heidelberg: Berlin, Heidelberg, 2013; Vol. pp 125-171.

- (19) Carpentier, J.-F.; Liu, B.; Sarazin, Y. In *Advances in Organometallic Chemistry and Catalysis*, John Wiley & Sons, Inc.: 2013; Vol. pp 359-378.
- (20) dos Santos Vieira, I.; Herres-Pawlis, S. *Eur. J. Inorg. Chem.* **2012**, *2012*, 765-774.
- (21) Wheaton, C. A.; Hayes, P. G. *Comments Inorg. Chem.* **2011**, *32*, 127-162.
- (22) Inkinen, S.; Hakkarainen, M.; Albertsson, A.-C.; Södergård, A. *Biomacromolecules* **2011**, *12*, 523-532.
- (23) Dutta, S.; Hung, W.-C.; Huang, B.-H.; Lin, C.-C. In *Synthetic Biodegradable Polymers*, Rieger, B.; Künkel, A.; Coates, G. W.; Reichardt, R.; Dinjus, E.; Zevaco, T. A., Eds. Springer-Verlag: Berlin, 2011; Vol. pp 219-284.
- (24) Dijkstra, P. J.; Du, H.; Feijen, J. *Polym. Chem.* **2011**, *2*, 520-527.
- (25) Dagorne, S.; Fliedel, C.; de Frémont, P. In *Encyclopedia of Inorganic and Bioinorganic Chemistry*, John Wiley & Sons, Ltd: 2011; Vol.
- (26) Buffet, J.-C.; Okuda, J. *Polym. Chem.* **2011**, *2*, 2758-2763.
- (27) Thomas, C. M. *Chem. Soc. Rev.* **2010**, *39*, 165.
- (28) Stanford, M. J.; Dove, A. P. *Chem. Soc. Rev.* **2010**, *39*, 486-494.
- (29) Jones, M. D. In *Heterogenized Homogeneous Catalysts for Fine Chemicals Production*, Barbaro, P.; Liguori, F., Eds. Springer Netherlands: 2010; Vol. 33, pp 385-412.
- (30) Ajellal, N.; Carpentier, J.-F.; Guillaume, C.; Guillaume, S. M.; Helou, M.; Poirier, V.; Sarazin, Y.; Trifonov, A. *Dalton Trans.* **2010**, *39*, 8363.
- (31) Wheaton, C. A.; Hayes, P. G.; Ireland, B. J. *Dalton Trans.* **2009**, 4832 - 4846.
- (32) Sun, J.; Shi, W.; Chen, D.; Liang, C. *J. Appl. Polym. Sci.* **2002**, *86*, 3312-3315.
- (33) John, A.; Katiyar, V.; Pang, K.; Shaikh, M. M.; Nanavati, H.; Ghosh, P. *Polyhedron* **2007**, *26*, 4033-4044.
- (34) Bhunora, S.; Mugo, J.; Bhaw-Luximon, A.; Mapolie, S.; Van Wyk, J.; Darkwa, J.; Nordlander, E. *Appl. Organomet. Chem.* **2011**, *25*, 133-145.
- (35) Chen, L.-L.; Ding, L.-Q.; Zeng, C.; Long, Y.; Lü, X.-Q.; Song, J.-R.; Fan, D.-D.; Jin, W.-J. *Appl. Organomet. Chem.* **2011**, *25*, 310-316.
- (36) Gowda, R. R.; Chakraborty, D. *J. Molec. Catal. A: Chem.* **2011**, *349*, 86-93.
- (37) Li, C.-Y.; Hsu, S.-J.; Lin, C.-I.; Tsai, C.-Y.; Wang, J.-H.; Ko, B.-T.; Lin, C.-H.; Huang, H.-Y. *J. Polym. Sci., Part A: Polym. Chem.* **2013**, *51*, 3840-3849.
- (38) Appavoo, D.; Omondi, B.; Guzei, I. A.; van Wyk, J. L.; Zinyemba, O.; Darkwa, J. *Polyhedron* **2014**, *69*, 55-60.
- (39) Akpan, E. D.; Ojwach, S. O.; Omondi, B.; Nyamori, V. O. *New J. Chem.* **2016**, *40*, 3499-3510.
- (40) Mandal, M.; Oppelt, K.; List, M.; Teasdale, I.; Chakraborty, D.; Monkowius, U. *Monatsh. Chem.* **2016**, *147*, 1883-1892.
- (41) Routaray, A.; Nath, N.; Maharana, T.; Sahoo, P. K.; Das, J. P.; Sutar, A. K. *J Chem Sci* **2016**, *128*, 883-891.
- (42) Ahn, S. H.; Chun, M. K.; Kim, E.; Jeong, J. H.; Nayab, S.; Lee, H. *Polyhedron* **2017**, *127*, 51-58.
- (43) Chun, M. K.; Cho, J.; Nayab, S.; Jeong, J. H. *Bull. Korean Chem. Soc.* **2017**, *38*, 1527-1530.
- (44) Kwon, K. S.; Nayab, S.; Jeong, J. H. *Polyhedron* **2017**, *130*, 23-29.
- (45) Cho, J.; Nayab, S.; Jeong, J. H. *Polyhedron* **2016**, *113*, 81-87.
- (46) Kwon, K. S.; Cho, J.; Nayab, S.; Jeong, J. H. *Inorg. Chem. Commun.* **2015**, *55*, 36-38.
- (47) Daneshmand, P.; Jiménez-Santiago, J. L.; Aragon-Alberti, M.; Schaper, F. *Organometallics* **2018**, *37*, 1751-1759.
- (48) Daneshmand, P.; Randimbiarisolo, A.; Schaper, F. *Can. J. Chem.* **2018**, *in print*,
- (49) Daneshmand, P.; Fortun, S.; Schaper, F. *Organometallics* **2017**, *36*, 3860-3877.

- (50) Daneshmand, P.; van der Est, A.; Schaper, F. *ACS Catal.* **2017**, *7*, 6289-6301.
- (51) Whitehorne, T. J. J.; Schaper, F. *Can. J. Chem.* **2014**, *92*, 206-214.
- (52) Whitehorne, T. J. J.; Schaper, F. *Inorg. Chem.* **2013**, *52*, 13612-13622.
- (53) Whitehorne, T. J. J.; Schaper, F. *Chem. Commun. (Cambridge, U. K.)* **2012**, *48*, 10334-10336.
- (54) Hardouin Duparc, V.; Schaper, F. *Organometallics* **2017**, *36*, 3053-3060.
- (55) Hardouin Duparc, V.; Thouvenin, A.; Schaper, F. *unpublished results* **2018**,
- (56) Hardouin Duparc, V.; Schaper, F. *Dalton Trans.* **2017**, *46*, 12766 - 12770.
- (57) Hardouin Duparc, V.; Bano, G. L.; Schaper, F. *ACS Catal.* **2018**, *8*, 7308-7325.
- (58) Chan, D. M. T.; Monaco, K. L.; Wang, R.-P.; Winters, M. P. *Tetrahedron Lett.* **1998**, *39*, 2933-2936.
- (59) Evans, D. A.; Katz, J. L.; West, T. R. *Tetrahedron Lett.* **1998**, *39*, 2937-2940.
- (60) Lam, P. Y. S.; Clark, C. G.; Saubern, S.; Adams, J.; Winters, M. P.; Chan, D. M. T.; Combs, A. *Tetrahedron Lett.* **1998**, *39*, 2941-2944.
- (61) Bhunia, S.; Pawar, G. G.; Kumar, S. V.; Jiang, Y.; Ma, D. *Angew. Chem., Int. Ed.* **2017**, *56*, 16136-16179.
- (62) Lam, P. Y. S. In *Synthetic Methods in Drug Discovery: Volume 1*, The Royal Society of Chemistry: 2016; Vol. 1, pp 242-273.
- (63) Neuville, L. In *Copper-Mediated Cross-Coupling Reactions*, John Wiley & Sons, Inc.: 2013; Vol. pp 113-185.
- (64) Casitas, A.; Ribas, X. In *Copper-Mediated Cross-Coupling Reactions*, John Wiley & Sons, Inc.: 2013; Vol. pp 253-279.
- (65) Allen, S. E.; Walvoord, R. R.; Padilla-Salinas, R.; Kozlowski, M. C. *Chem. Rev.* **2013**, *113*, 6234-6458.
- (66) Sanjeeva Rao, K.; Wu, T.-S. *Tetrahedron* **2012**, *68*, 7735-7754.
- (67) Rauws, T. R. M.; Maes, B. U. W. *Chem. Soc. Rev.* **2012**, *41*, 2463-2497.
- (68) Beletskaya, I. P.; Cheprakov, A. V. *Organometallics* **2012**, *31*, 7753-7808.
- (69) Qiao, J. X.; Lam, P. Y. S. In *Boronic Acids*, Wiley-VCH Verlag GmbH & Co. KGaA: 2011; Vol. pp 315-361.
- (70) Bellina, F.; Rossi, R. *Adv. Synth. Catal.* **2010**, *352*, 1223-1276.
- (71) Evano, G.; Blanchard, N.; Toumi, M. *Chem. Rev.* **2008**, *108*, 3054-3131.
- (72) Ley, S. V.; Thomas, A. W. *Angew. Chem., Int. Ed.* **2003**, *42*, 5400-5449.
- (73) Bag, B.; Mondal, N.; Mitra, S.; Gramlich, V.; Ribas, J.; El Fallah, M. S. *Polyhedron* **2001**, *20*, 2113-2116.
- (74) Dey, S. K.; Bag, B.; Abdul Malik, K. M.; El Fallah, M. S.; Ribas, J.; Mitra, S. *Inorg. Chem.* **2003**, *42*, 4029-4035.
- (75) Sasmal, A.; Garribba, E.; Rizzoli, C.; Mitra, S. *Inorg. Chem.* **2014**, *53*, 6665-6674.
- (76) Nakao, Y.; Yamazaki, M.; Suzuki, S.; Mori, W.; Nakahara, A.; Matsumoto, K.; Ooi, S. I. *Inorg. Chim. Acta* **1983**, *74*, 159-167.
- (77) Colacio, E.; Ghazi, M.; Kivekäs, R.; Moreno, J. M. *Inorg. Chem.* **2000**, *39*, 2882-2890.
- (78) Shi, W.-J. *Acta Crystallogr., Sect. C* **2009**, *65*, m284-m286.
- (79) Leong, W. L.; Vittal, J. J. *Journal of Inclusion Phenomena and Macrocyclic Chemistry* **2011**, *71*, 557-566.
- (80) The provided NMR data differed from the one we obtained later for this product and resembled closely those of the starting materials.
- (81) Nitschke, J. R. *Angew. Chem., Int. Ed.* **2004**, *43*, 3073-3075.
- (82) Ou, Y.-M.; Zhao, Z.-Y.; Yue-Hua Shi; Zhang, Y.-L.; Jiang, Y.-M. *Chin. J. Struct. Chem.* **2009**, *28*, 457.

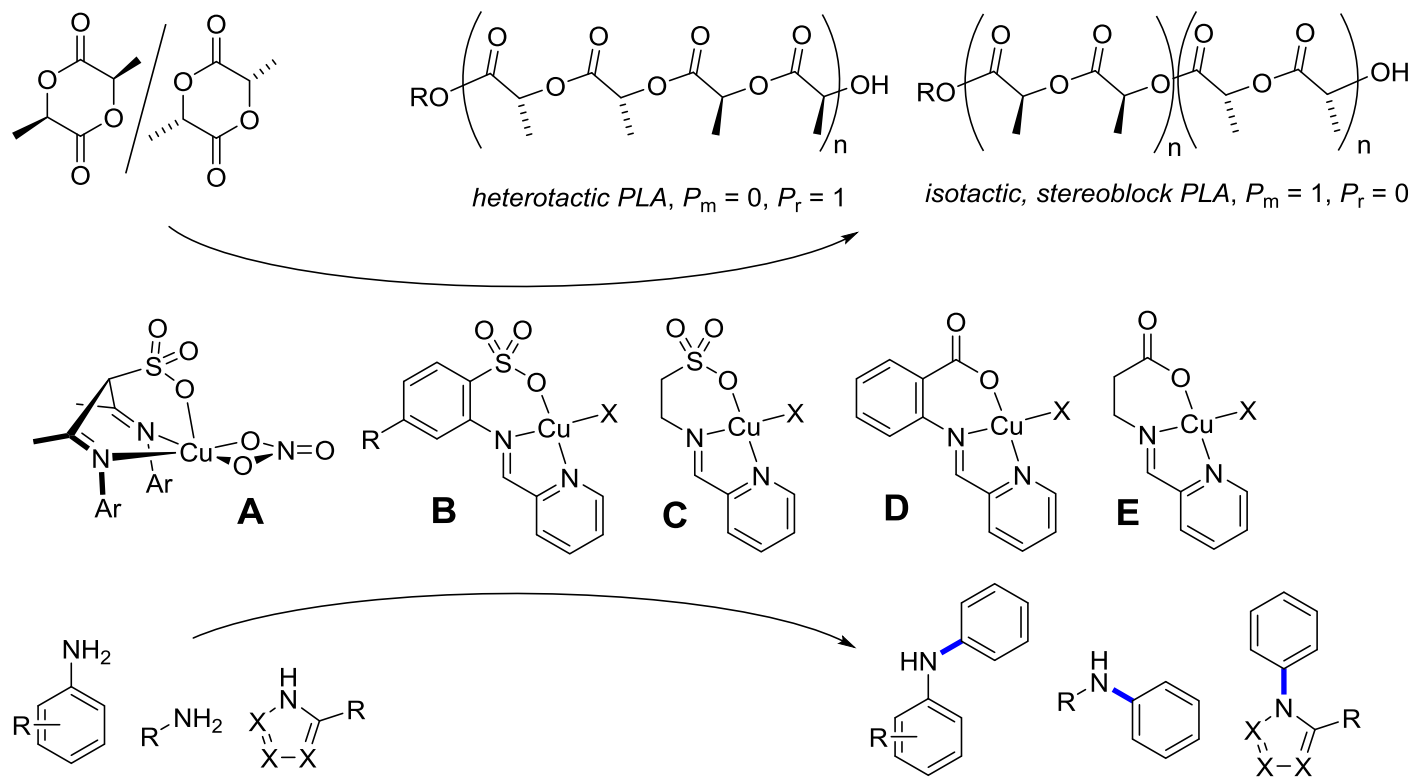
- (83) The crystal structure of the nitrate complex was determined to verify composition, as for all the other complexes. Since the original structure determination was conducted at room temperature, we included the low temperature data obtained here in the supporting information.
- (84) Qiu, C.-J.; Zhang, Y.-C.; Gao, Y.; Zhao, J.-Q. *J. Organomet. Chem.* **2009**, *694*, 3418-3424.
- (85) Harding, P.; Harding, D. J.; Soponrat, N.; Tinpun, K.; Samuadnuan, S.; Adams, H. *Aust. J. Chem.* **2010**, *63*, 75-82.
- (86) Culkun Darcy, A.; Jeong, W.; Csihony, S.; Gomez Enrique, D.; Balsara Nitash, P.; Hedrick James, L.; Waymouth Robert, M. *Angew. Chem.* **2007**, *119*, 2681-2684.
- (87) Antilla, J. C.; Buchwald, S. L. *Org. Lett.* **2001**, *3*, 2077-2079.
- (88) Quach, T. D.; Batey, R. A. *Org. Lett.* **2003**, *5*, 1381-1384.
- (89) King, A. E.; Ryland, B. L.; Brunold, T. C.; Stahl, S. S. *Organometallics* **2012**, *31*, 7948-7957.
- (90) Collman, J. P.; Zhong, M.; Zhang, C.; Costanzo, S. *J. Org. Chem.* **2001**, *66*, 7892-7897.
- (91) Vantourout, J. C.; Miras, H. N.; Isidro-Llobet, A.; Sproules, S.; Watson, A. J. B. *J. Am. Chem. Soc.* **2017**, *139*, 4769-4779.
- (92) Save, M.; Schappacher, M.; Soum, A. *Macromol. Chem. Phys.* **2002**, *203*, 889-899.
- (93) *Apex2*, Release 2.1-0; Bruker AXS Inc.: Madison, USA, 2006.
- (94) *Saint*, Release 7.34A; Bruker AXS Inc.: Madison, USA, 2006.
- (95) Sheldrick, G. M. *Sadabs*, Bruker AXS Inc.: Madison, USA, 1996 & 2004.
- (96) Sheldrick, G. *Acta Crystallogr. Sect. A: Found. Crystallogr.* **2015**, *71*, 3-8.
- (97) Sheldrick, G. M. *Acta Crystallogr.* **2008**, *A64*, 112-122.

**Figure 1.** X-ray structures (from left to right) of **1**, **3**, **4** and **5**. Thermal ellipsoids are drawn at the 50% probability level. Hydrogen atoms and co-crystallized water (**1**, **3**, **4**) and the nitrate anion (**3**) omitted for clarity. The inset shows the 1D coordination polymer (**5**)<sub>n</sub> (see also Fig. S5)

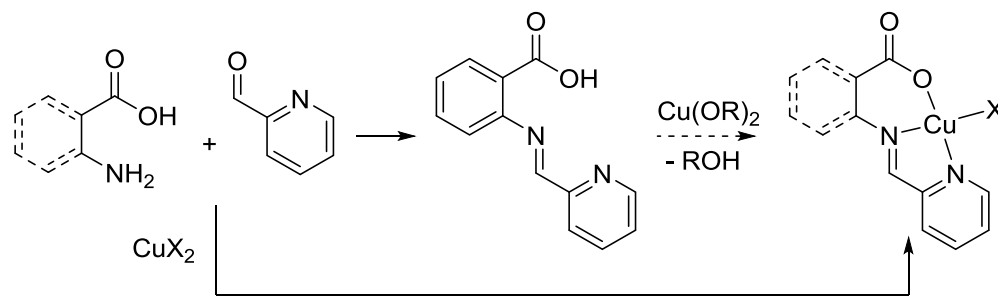
**Figure 2.** Crystal structures of **6** and **7**. Thermal ellipsoids are shown at 50% probability. Hydrogen atoms omitted for clarity.

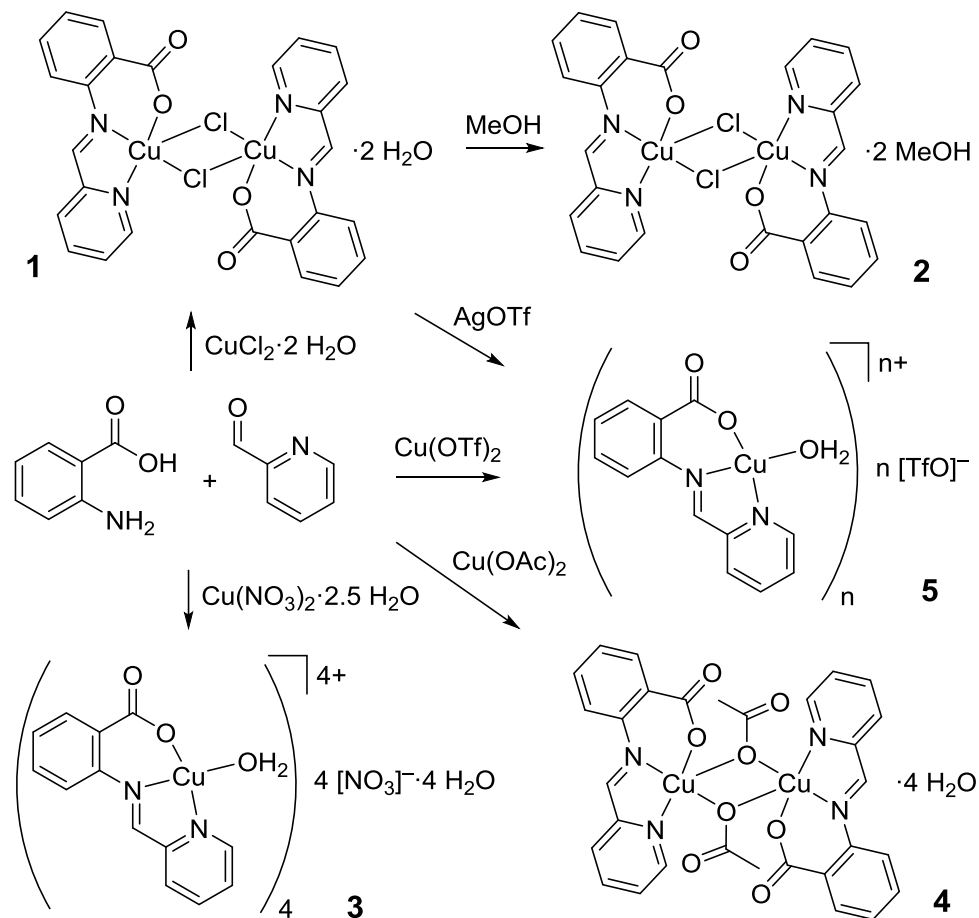
**Figure 3.** UV/vis spectra of **1** - **7** in DMSO

**Figure 4.** Concentration-time profiles for CEL couplings of cyclohexylamine with phenylboronic acid, catalyzed by **1-6**. Conditions: 1.0 M cyclohexylamine, 1.5 M PhB(OH)<sub>2</sub>, 2.5 mol% catalyst, MeOH, RT, air. Conversion was calculated from absolute concentrations of product and starting material, obtained by calibrated GC-MS analyses vs. internal standard. The solid lines are theoretical conversions using the pseudo-first-order rate constants determined by linear regression of the semilogarithmic plot.

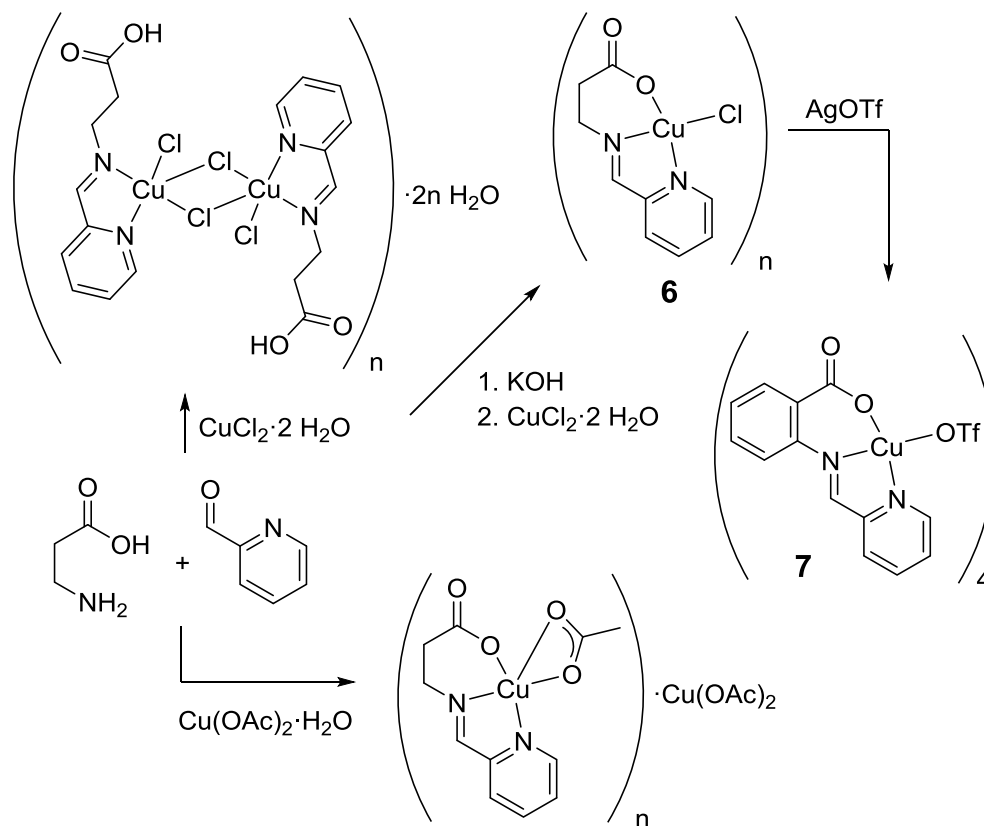


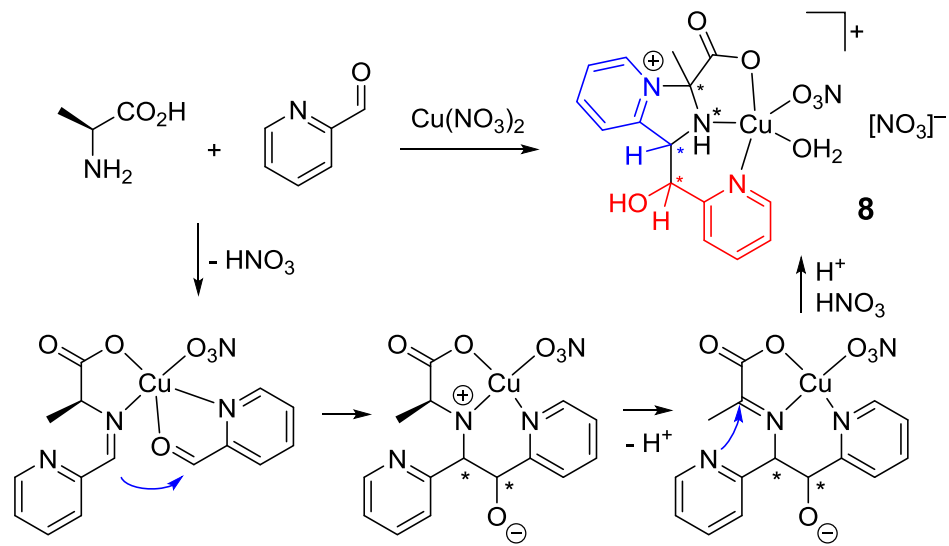
Scheme 1

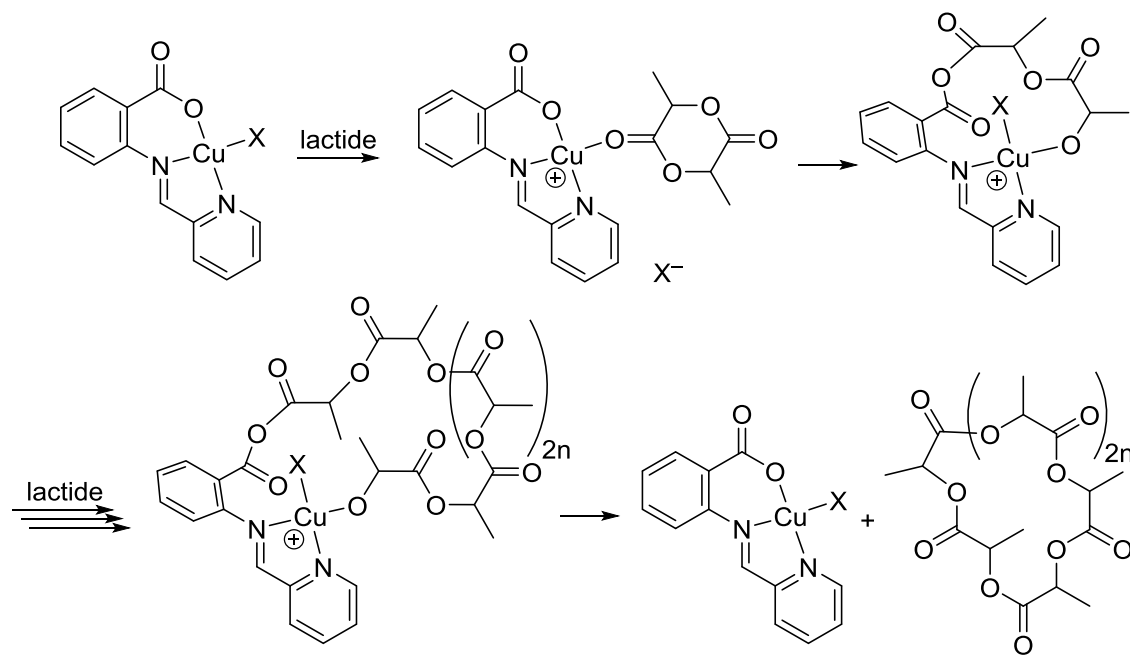


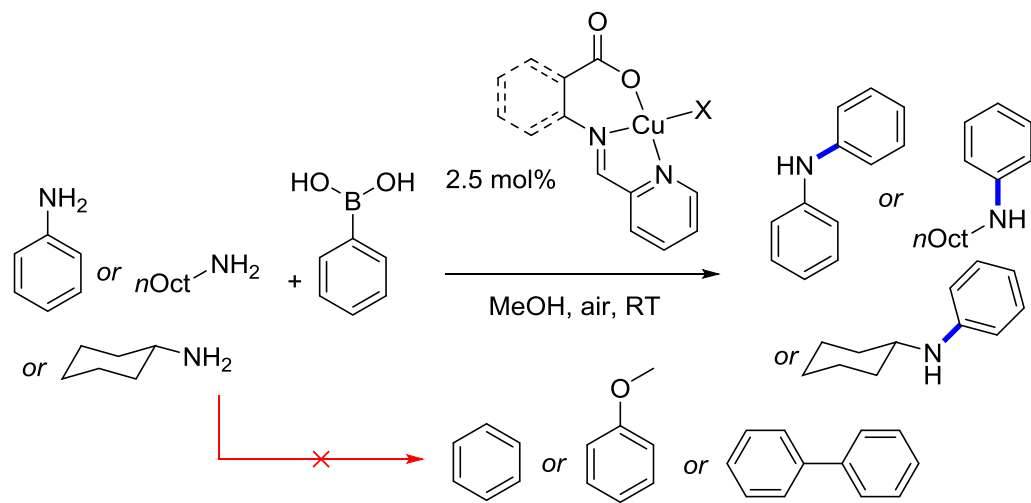


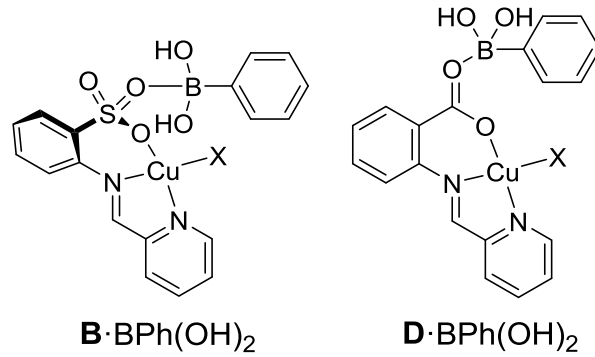
Scheme 3











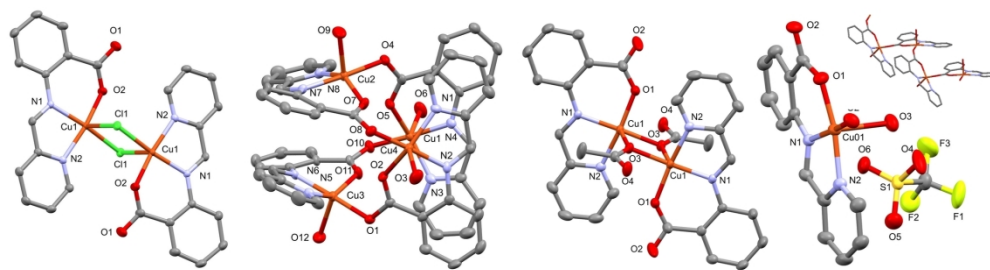


Figure 1

181x48mm (300 x 300 DPI)

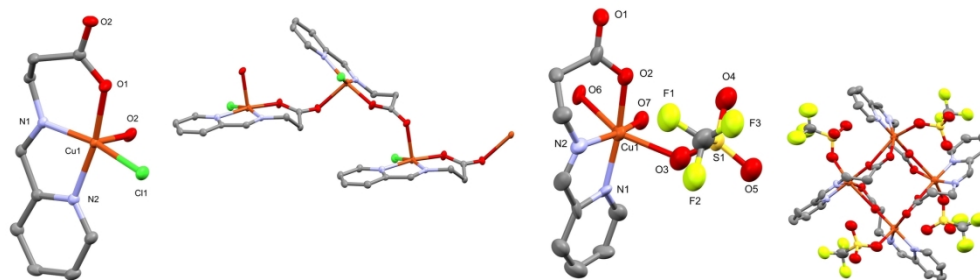


Figure 2

181x52mm (300 x 300 DPI)

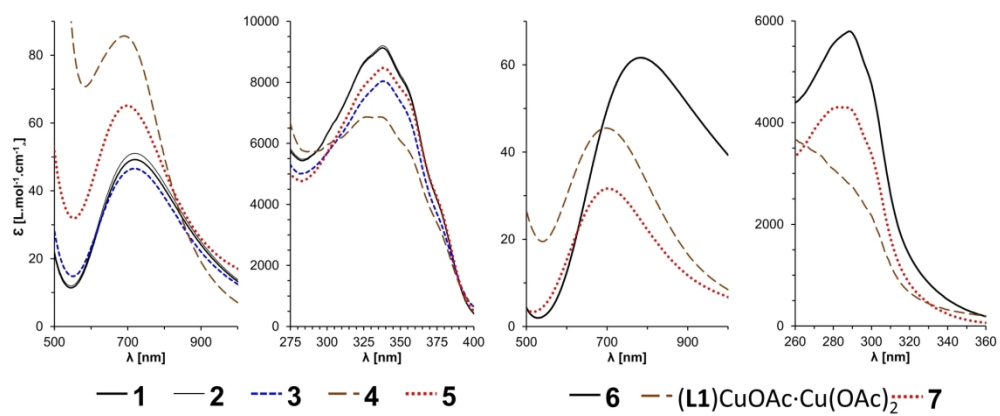


Figure 3

181x75mm (300 x 300 DPI)

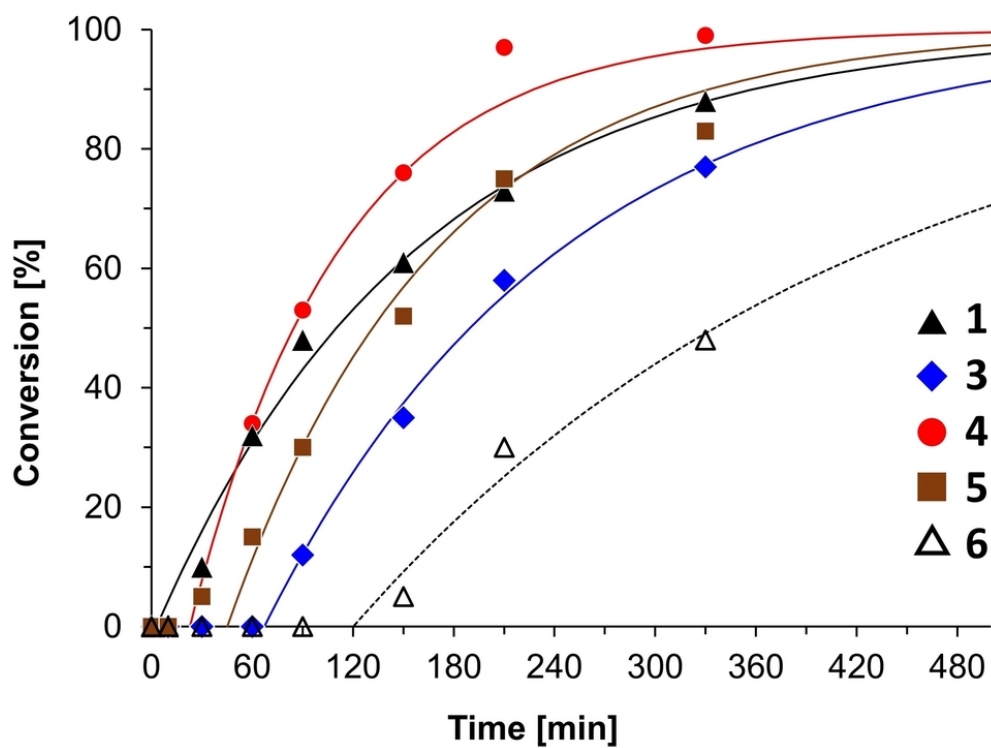


Figure 4

81x60mm (300 x 300 DPI)